Global calculation of α-decay half-lives with a deformed density-dependent cluster model

Chang Xu[1] and Zhongzhou Ren[1,2,3,*]
[1]*Department of Physics, Nanjing University, Nanjing 210008, China*
[2]*Center of Theoretical Nuclear Physics, National Laboratory of Heavy-Ion Accelerator, Lanzhou 730000, China*
[3]*CPNPC, Nanjing University, Nanjing 210008, China*
(Received 13 April 2006; published 11 July 2006)

A global calculation of favored α-decay half-lives of both even-A and odd-A deformed nuclei is carried out in the framework of a deformed version of the density-dependent cluster model (DDCM). The influence of nuclear deformation on α-decay half-lives is taken into account in the deformed DDCM. The microscopic potential between the spherical α particle and the deformed daughter nucleus is evaluated numerically from the double-folding model by the multipole expansion method. The deformation and orientation dependence of the α-core potential is analyzed and discussed. The formulas of the deformed DDCM are presented in detail, and a large number of numerical calculations of medium and heavy nuclei with available data are completed. The total number of α emitters calculated in this article is 485, and this covers the nuclei with $Z = 52$–110. This is a complete study of α-decay half-lives on both even-A and odd-A nuclei with deformed microscopic potentials. The numerical results obtained by the deformed DDCM are in good agreement with the experimental data.

DOI: 10.1103/PhysRevC.74.014304 PACS number(s): 23.60.+e, 21.10.Tg, 21.60.−n, 24.10.−i

I. INTRODUCTION

The ground state of unstable nuclei has been observed to have different kinds of decay modes: α decay, β decay, proton emission, and spontaneous fission. α decay is one of the most important decay modes for nuclei with proton numbers $Z \geqslant 52$. Measurements on α decay of ground-state nuclei can provide reliable information on nuclear structure such as ground-state energy, ground-state lifetime, and nuclear spin and parity. Measurements on α decay are also used to identify new nuclides or new elements because α decay is a clean and reliable mode to extract information on the parent nuclei [1–9]. To date, there are more than 400 nuclei in the periodic table that exhibit the α-decay phenomenon [1,2]. In recent years, there has been renewed interest in α decay because of the development of radioactive beams and new detector technology under low temperature [3,4]. Thanks to these new developments, α decay is now a powerful tool for investigating the details of nuclear structure, e.g., α clustering, shell effect, effective nuclear interaction, and nuclear deformation [10–15]. From the theoretical side, the process of α decay is fundamentally a quantum-tunneling effect, which was first explained by Gamow and by Condon and Guerney in the 1920s [16,17]. This pioneering work proved the correctness of quantum mechanics for nuclear phenomena and led to the use of quantum mechanics on nuclear many-body systems. Subsequently, a number of theoretical calculations were performed to predict absolute α decay width, to extract nuclear structure information, and to pursue a microscopic understanding of α-decay phenomenon. These studies are based on various theoretical models such as the shell model, fissionlike model, and cluster model [18–29]. Recently, we studied favored α-decay half-lives for two different mass regions with the spherical version of the density-dependent cluster model (DDCM) [30]. To simplify the multidimensional problem, we assumed a spherical shape for both the parent and daughter nuclei in previous calculations [30]. Indeed, we know that many ground-state α emitters are spherical or moderately deformed [31,32]. Many different spherical treatments obtained similar results for favored α-decay half-lives [21–29]. Although the spherical model has been successful to some extent, it is useful to work beyond the spherical approximation and to include new factors such as nuclear deformation [33–35]. Very recently, we included the deformation effect on α decay half-lives and proposed the deformed version of the DDCM [36]. The results of even-even nuclei have already been reported [36]. In this article, we present detailed formulas of the deformed DDCM and extend our calculation to both odd-A nuclei and odd-odd nuclei in a wide mass region $Z = 52-110$. In the deformed DDCM, the microscopic deformation- and orientation-dependent α-core potentials are evaluated numerically from the double-folding model by the multipole expansion method [37–40]. Such nonspherical double-folding potentials are difficult to calculate by common Fourier transformation techniques and have rarely been used in the calculation of α-decay half-lives [37,38]. We analyze and discuss the deformation and orientation dependence of the α-core potentials in detail. Much computational time is required when the influence of nuclear deformation of the daughter nucleus is taken into account. The number of α emitters calculated in this article is 485. The numerical results of the favored α transitions by the deformed DDCM are systematically compared with the available experimental data.

The outline of this paper is as follows. In Sec. II, we present the formulas and parameters of the deformed version of the density-dependent cluster model. The numerical results and corresponding discussions for even-A, odd-A, and superheavy nuclei are given in Sec. III. Section IV is a summary.

*Electronic address: zren@nju.edu.cn

II. DENSITY-DEPENDENT CLUSTER MODEL OF α DECAY

In the density-dependent cluster model, the ground state of the parent nucleus is assumed to be an α particle interacting with the daughter nucleus. The expression of α decay width in the spherical DDCM is [21,30]

$$\Gamma = P_\alpha F \frac{\hbar^2}{4\mu} \exp\left[-2\int_{R_2}^{R_3} dR \sqrt{\frac{2\mu}{\hbar^2}|Q - V(R)|}\right], \quad (1)$$

where P_α is the preformation probability of the α particle in the parent nucleus and F is the normalization factor [21,30]. μ is the reduced mass of the α-core system, and Q is the experimental α decay energy. The total α-core potential $V(R)$ consists of the nuclear potential, Coulomb potential, and centrifugal potential. The spherical expression of α decay width was proposed by Gurvitz and Kalbermann [20] based on the two-potential approach (TPA). This expression is widely used in the spherical calculations of α decay width [21,22]. To extend the α decay width to the deformed case, we assume a spherical α-particle interacts with an axially symmetric deformed daughter nucleus. The total α-core potential is given by [30]

$$V_{\text{Total}}(R,\beta) = V_N(R,\beta) + V_C(R,\beta) + \frac{\hbar^2}{2\mu}\frac{(L+\frac{1}{2})^2}{R^2}, \quad (2)$$

where R is the separation between the mass center of the α particle and the mass center of the core. β is the orientation angle of the α particle with respect to the symmetry axis of the daughter nucleus. Usually the centrifugal term is written in the form $(L+\frac{1}{2})^2$ in the semiclassical approximation [21,30]. When the term $L(L+1)$ is replaced by the term $(L+\frac{1}{2})^2$, there is no significant variation for α decay half-lives of nuclei [21,30]. The nuclear and Coulomb potentials are obtained from the double-folding model [41–43]

$$V_{N\,\text{or}\,C}(R,\beta) = \int d\mathbf{r_1} d\mathbf{r_2} \rho_1(\mathbf{r_1})\rho_2(\mathbf{r_2})v(\mathbf{s}), \quad (3)$$

where ρ_1 and ρ_2 are the density distributions of the α particle and the daughter nucleus, respectively [37,42]. $v(\mathbf{s})$ is the effective nucleon-nucleon interaction. The quantity $|\mathbf{s}|$ is the distance between a nucleon in the core and a nucleon in the α particle: $\mathbf{s} = \mathbf{R} + \mathbf{r}_2 - \mathbf{r}_1$ [37,42]. The coordinates used in the double-folding model are defined by Fig. 1. The mass

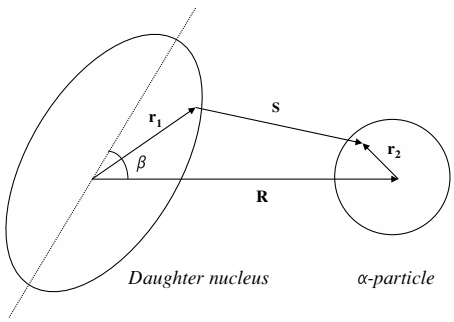

FIG. 1. Schematic explanation of coordinates used in double-folding model.

density distribution of the spherical α particle ρ_1 is a standard Gaussian form given by Satchler and Love [37]. The mass density distribution of the daughter nucleus ρ_2 is a deformed Fermi distribution and the values of parameters are taken from the standard textbooks [44,45]. The mass density distribution of the daughter nucleus is written as

$$\rho_2(r_2,\theta) = \frac{\rho_0}{1+\exp[\frac{r_2 - R(\theta)}{a}]}, \quad (4)$$

where the value of ρ_0 is fixed by integrating the density distribution equivalent to the mass number of the daughter nucleus A_d. The half-density radius $R(\theta)$ is given by

$$R(\theta) = R_0[1 + \beta_2 Y_{20}(\theta) + \beta_4 Y_{40}(\theta)], \quad (5)$$

where the parameters $R_0 = 1.07A_d^{1/3}$ fm and $a = 0.54$ fm are taken from [44,45]. When $\beta_2 = \beta_4 = 0$, the matter radius of heavy nuclei with this choice is $R_{\text{rms}} \approx 1.2 \times A^{1/3}$ (fm) and this is back to the spherical case automatically [44,45]. The famous M3Y-Reid type nucleon-nucleon interaction and the standard proton-proton Coulomb interaction are used in DDCM. The M3Y interaction was first proposed by Bertsch *et al.* which was derived from the G-matrix elements of the Reid potential [41]. It is given by two direct terms with different ranges and by an exchange term with a delta interaction, and the parametrized form is given by Satchler and Love [37]

$$v(\mathbf{s}) = 7999\frac{\exp(-4s)}{4s} - 2134\frac{\exp(-2.5s)}{2.5s} + J_{00}\delta(\mathbf{s}), \quad (6)$$
$$J_{00} = -276(1 - 0.005E_\alpha/A_\alpha),$$

where E_α is the α-decay energy and A_α is the mass number of the α particle. The energy dependence of the exchange term is actually very weak for the α decay energies ranged mainly from 2 to 12 MeV. The double-folding potential in the deformed case involves a complex six-dimensional integral. For the spherical-deformed interacting pair, the double-folding potential is solved numerically by using the multipole expansion method in which the density distribution of the daughter nucleus is expanded as [39,40]

$$\rho(r,\theta) = \sum_{l=0,2,4\ldots} \rho_l(r) Y_{l0}(\theta). \quad (7)$$

The corresponding intrinsic form factor has the form [39]

$$\tilde{\rho}^{(l)}(k) = \int_0^\infty dr r^2 \rho_l(r) j_l(kr). \quad (8)$$

The double-folding potential can be evaluated by a sum of different multipole components [39]

$$V_{N\,\text{or}\,C}(R,\beta) = \sum_{l=0,2,4\ldots} V^l_{N\,\text{or}\,C}(R,\beta), \quad (9)$$

and the multipole component of the double-folding potential is given by

$$V^l_{N\,\text{or}\,C}(R,\beta) = \frac{2}{\pi}[(2l+1)/4\pi]^{1/2} \times \int_0^\infty dk k^2 j_l(kR)\tilde{\rho}_1(k)\tilde{\rho}_2{}^{(l)}(k)\tilde{v}(k)P_l(\cos\beta), \quad (10)$$

where $\tilde{\rho}_1(k)$ is the Fourier transformation of the density distribution of the α particle. $\tilde{\rho}_2^{(l)}(k)$ is the intrinsic form factor [Eq. (8)]. $\tilde{v}(k)$ is the Fourier transformation of a local two-body effective interaction. $P_l(\cos\beta)$ is the Legendre function of degree l. The double-folding potentials given by Eqs. (9) and (10) are functions of both the separation R and the orientation angle β (see Fig. 1). We note that the depth of the double-folding nuclear potential is determined separately for each decay to ensure the quasibound condition [21,30]

$$\int_0^{\pi}\int_{R_1(\beta)}^{R_2(\beta)}\sqrt{\frac{2\mu}{\hbar^2}[Q - V_{\text{Total}}(R,\beta)]}\sin\beta dR d\beta = (G - L + 1)\frac{\pi}{2}, \tag{11}$$

where $R_1(\beta)$, $R_2(\beta)$, and $R_3(\beta)$ are three classical turning points of a certain orientation angle β. The values of $R_1(\beta)$, $R_2(\beta)$, and $R_3(\beta)$ are obtained by numerical solutions of the equation $V_{\text{Total}}(R,\beta) = Q$. L is the angular momentum carried by the α particle, and G is the global quantum number given by [30]

$$\begin{aligned} G &= 20(N > 126),\\ G &= 18(82 < N \leqslant 126),\\ G &= 16(N \leqslant 82). \end{aligned} \tag{12}$$

It is interesting to note that the depth of the nuclear potential, i.e., the renormalization factor λ, is not an adjusting parameter in DDCM [30]. It is chosen to generate a quasistationary state with the global quantum numbers G and L [30]. In fact, the variation of λ is small in both spherical and deformed cases where its values range from $\lambda = 0.55$ to 0.65 for different nuclei. When the α-core interaction has been determined, the width Γ is calculated by the microscopic double-folding nuclear and Coulomb potentials. It is well known that in both spherical and deformed treatments, the magnitude of the α-decay width is mainly determined by the corresponding penetration probability. In the deformed DDCM, the polar-angle dependent penetration probability of α decay is given by

$$P_\beta = \exp\left[-2\int_{R_2(\beta)}^{R_3(\beta)}\sqrt{\frac{2\mu}{\hbar^2}|Q_\alpha - V_{\text{Total}}(R,\beta)|}dR\right], \tag{13}$$

where $R_2(\beta)$ and $R_3(\beta)$ are the second and third classical turning points for a certain orientation angle β. The total penetration factor P is obtained by averaging P_β in all directions such that

$$P = \frac{1}{2}\int_0^{\pi} P_\beta \sin(\theta)\, d\theta. \tag{14}$$

This averaging procedure is widely used in both α decay and fusion reaction calculations which can also be found in Refs. [33–35]. The value of the normalization factor F is also obtained by averaging along different orientation angles. This is similar to previous work, but now it is more complex [30]. From the numerical results, we know that the value of F in the deformed case is very close to that of the spherical one [30].

The α decay width in the deformed DDCM is given by [36]

$$\Gamma = P_\alpha F \frac{\hbar^2}{4\mu}\frac{1}{2}\int_0^{\pi} P_\beta \sin(\theta)\, d\theta. \tag{15}$$

The α decay half-life is related to the decay width by the well-known expression [30]

$$T_{1/2} = \hbar \ln 2/\Gamma. \tag{16}$$

III. THEORETICAL RESULTS AND DISCUSSIONS

A. Double-folding potential of the spherical-deformed nuclear pair

The microscopic α-core potential plays an important role in the calculation of α decay half-lives. Because the daughter nucleus has an axially symmetric shape, the nuclear and Coulomb potentials between α particle and daughter nucleus are actually nonspherical in deformed DDCM calculations. However, the calculation of the deformed double-folding potential is time consuming. It is found that the multipole expansion method is a good approximation for calculating the microscopic double-folding potentials between the spherical α particle and the deformed daughter nucleus. It is also proved in Ref. [40] that the multipole expansion is accurate and stable for the spherical-deformed nuclear pair. In our calculations, we use the standard proton-proton Coulomb interaction and the effective M3Y interaction which is derived from the Reid nucleon-nucleon potential [41]. In Fig. 2, we illustrate the sum of nuclear and Coulomb potentials of $\alpha+^{232}$Th system for two different orientations $\beta = 0^\circ$ and $\beta = 90^\circ$. The deformation of the daughter nucleus ^{232}Th is taken from Möller *et al.* [31]. We use their theoretical deformation because the value agrees well with the magnitude of experimental deformation [32]. The difference between the experimental deformation and that from Möller *et al.* is small, and its influence on the calculated half-lives is not large. For spherical nuclei, it is obvious that the shapes and depths of the obtained double-folding potentials are the same in all orientations and the calculated

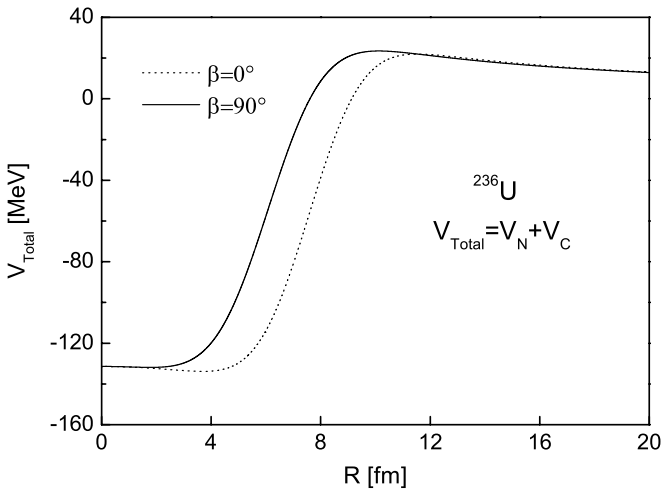

FIG. 2. Sum of double-folding nuclear and Coulomb potentials of ^{236}U for two orientations $\beta = 0^\circ$ and $\beta = 90^\circ$.

α-core interactions are only a function of the separation R. For deformed nuclei, the double-folding potentials are dependent on both the separation R and the orientation angle β. As shown in Fig. 2, the total potential at $\beta = 0^\circ$ is more attractive than that at $\beta = 90^\circ$ in the medium region. This is because there is a large overlap of nuclear density distribution at orientation angle $\beta = 0^\circ$. Larger deformation will certainly lead to more significant variations for different orientation angles. If the deformation parameter equals zero, the double-folding α-core potential is automatically back to that of the spherical case in DDCM.

B. Variation of each term in deformed DDCM

In DDCM, the nuclear and Coulomb potentials are microscopically determined using input parameters, such as the radius and the diffuseness, that are all taken from the classical nuclear textbooks [44]. The depth of the nuclear potential λ is adjusted to reproduce the experimental α decay energy by application of the Bohr-Sommerfeld condition. The only free parameter in DDCM is the preformation factor of the α particle in the parent nucleus. In spherical calculations, the preformation factor of the α cluster is chosen as 1.0 for even-even heavy nuclei. For odd-A nuclei and odd-odd nuclei, the preformation factors are slightly reduced in the calculations [30]. In the medium mass region, a set of relatively small values is chosen for the three kinds of nuclei [30]. Experiments have shown that the preformation factor varies smoothly in the open-shell region and has a value smaller than 1.0 [14]. The microscopic calculation gives a value of 0.3 for the α-cluster preformation factor of even-even nucleus ^{212}Po [19]. In present calculations, we find that the experimental α decay half-lives of a certain kind of nuclei (even-even, odd-A, or odd-odd nuclei) can be well reproduced by using the same preformation factor. This means both the medium mass α emitters and heavy ones can be well described in a consistent way by the deformed DDCM. Through a least-squares fit to the available experimental half-lives of nuclei with $Z = 52$–105, we obtain a set of parameters of the preformation factors: $P_\alpha = 0.38$ for even-even nuclei, $P_\alpha = 0.24$ for odd-A nuclei, and $P_\alpha = 0.13$ for odd-odd nuclei. These values agree with both the experimental facts and the microscopic calculations [14,19]. It also agrees with the popular idea that the nuclear ground state is described mainly by the single-particle motion of the shell model, and the α-cluster probability in the ground-state wave function is less than a half. In DDCM, other factors in the decay width, such as the normalization factor F, vary smoothly in the deformed case. But the penetration factor P varies significantly when the deformation effect of the daughter nucleus is taken into account. So the penetration factor is more sensitive to nuclear deformation than to other terms of the decay width [46–49]. It is thus concluded that nuclear deformation mainly affects the barrier penetration probability of the α particle.

C. Comparison of experimental α-decay half-lives with theoretical ones for different kinds of nuclei

Now we discuss the calculated results of α-decay half-lives within the framework of the deformed DDCM. The α-decay energy Q_α and the excitation energies of the daughter nucleus E^*_{L+} are all measured values from experiments [1,2,21]. The small effect of the electron shielding correction on decay energy Q_α is also included in a standard way [21,30]. The values of nuclear deformation are taken from Ref. [31] which correspond to those of the daughter nucleus. Although the hexadecapole deformation is small for many α emitters and its influence on α-decay width is marginal, it can be included in the systematic calculations of half-lives for nuclei with $Z = 52$–105. Detailed analysis of the experimental and theoretical α-decay half-lives is given for different kinds of nuclei.

1. Even-even nuclei

The ground-state spin and parity of all even-even nuclei is 0^+. The α decay of even-even nuclei mainly proceeds to the ground state of the daughter nucleus. Although the parent nucleus can also decay to the excited states of the daughter nucleus, this probability is very small in normal cases, and it can be neglected for a systematic calculation of half-lives of many nuclei [21,30,36]. The α decay between the ground states of even-even nuclei is a favored transition, which means that the angular momentum and parity of the α particle is 0^+. We plot the logarithms of the hindrance factors for all even-even nuclei in Fig. 3. The hindrance factor is defined as the ratio between the experimental and theoretical α-decay half-lives (HF $= T_{\text{Exp.}}/T_{\text{Cal.}}$). It is known experimentally that the magnitude of α-decay half-lives of the even-even nuclei varies in a very wide range from 10^{-8} to 10^{24} s. Although the amplitude of the variation of half-lives is as high as 10^{32} times, we can see from Fig. 3 that the experimental α decay half-lives of many even-even nuclei are reproduced within a factor of 2 by the deformed DDCM [36].

Because we discussed the results of even-even nuclei in Ref. [30], we present here only a few typical results of even-even nuclei as a supplement to the previous publication. For even-even isotopic chains, the α-decay half-lives of the isotopes generally increase with increasing neutron number. However, for the trans-Pb isotopic chains, a sharp decrease of half-life occurs at the spherical shell closure $N = 126$. For instance, the α-decay half-life of the nucleus ^{210}Po is as

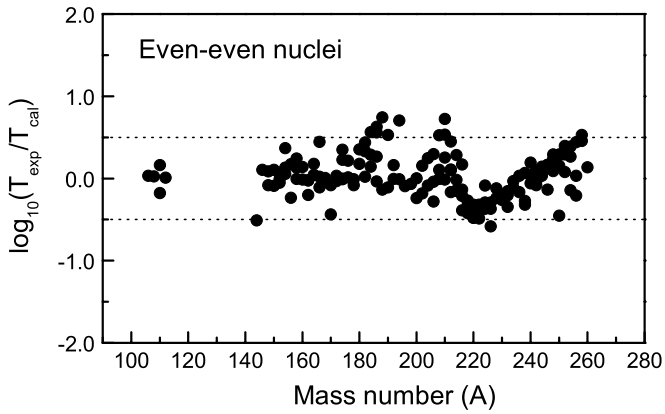

FIG. 3. Logarithms of hindrance factors (HF $= T_{\text{Exp.}}/T_{\text{Cal.}}$) of even-even nuclei ($Z = 52$–$104$).

TABLE I. Experimental and theoretical α-decay half-lives T (in log base 10 and in seconds) for even-even nuclei ($Z = 82$–88), where the nuclear deformation effect is taken into account.

A_p	Z_p	A_d	Z_d	Q_α(MeV)	β_2	β_4	$T_{\text{Exp.}}$	$T_{\text{Cal.}}$
182	Pb	178	Hg	7.054	−0.113	−0.026	−1.222	−1.243
184	Pb	180	Hg	6.807	−0.122	−0.026	−0.260	−0.403
186	Pb	182	Hg	6.505	−0.122	−0.018	0.681	0.716
188	Pb	184	Hg	6.141	−0.130	−0.017	2.041	2.176
190	Pb	186	Hg	5.731	−0.130	−0.025	3.903	4.013
192	Pb	188	Hg	5.252	−0.130	−0.025	6.602	6.441
194	Pb	190	Hg	4.766	−0.130	−0.032	9.996	9.290
210	Pb	206	Hg	3.823	−0.008	0.000	16.568	16.033
192	Po	188	Pb	7.354	0.000	−0.008	−1.469	−1.462
194	Po	190	Pb	7.022	0.000	−0.008	−0.357	−0.348
196	Po	192	Pb	6.688	0.000	−0.008	0.778	0.873
198	Po	194	Pb	6.341	0.000	−0.008	2.176	2.243
200	Po	196	Pb	6.014	0.000	−0.008	3.663	3.660
202	Po	198	Pb	5.733	0.000	−0.008	5.114	4.960
204	Po	200	Pb	5.516	0.000	−0.008	6.279	6.033
206	Po	202	Pb	5.358	0.000	−0.008	7.146	6.848
208	Po	204	Pb	5.248	−0.008	−0.008	7.959	7.433
210	Po	206	Pb	5.439	−0.008	−0.008	7.079	6.354
212	Po	208	Pb	8.985	0.000	0.000	−6.523	−6.633
214	Po	210	Pb	7.865	0.000	0.008	−3.796	−3.644
216	Po	212	Pb	6.939	0.000	0.008	−0.824	−0.613
218	Po	214	Pb	6.147	0.000	0.009	2.279	2.548
200	Rn	196	Po	7.083	0.000	0.015	0.000	0.238
202	Rn	198	Po	6.803	0.000	−0.015	1.079	1.260
204	Rn	200	Po	6.578	0.009	−0.015	2.041	2.127
206	Rn	202	Po	6.415	0.009	−0.015	2.740	2.780
208	Rn	204	Po	6.293	0.009	−0.015	3.380	3.274
210	Rn	206	Po	6.190	−0.018	−0.008	3.954	3.700
212	Rn	208	Po	6.413	−0.018	−0.008	3.146	2.698
214	Rn	210	Po	9.242	0.000	0.008	−6.569	−6.553
216	Rn	212	Po	8.235	0.000	0.008	−4.347	−3.959
218	Rn	214	Po	7.299	−0.008	0.008	−1.456	−1.035
220	Rn	216	Po	6.438	0.020	0.018	1.748	2.223
222	Rn	218	Po	5.623	0.039	0.028	5.519	6.004
206	Ra	202	Rn	7.450	−0.104	0.004	−0.620	−0.338
208	Ra	204	Rn	7.307	−0.087	0.003	0.146	0.152
210	Ra	206	Rn	7.190	−0.044	−0.007	0.568	0.581
212	Ra	208	Rn	7.068	−0.026	−0.008	1.114	1.013
214	Ra	210	Rn	7.306	−0.026	−0.008	0.398	0.114
216	Ra	212	Rn	9.559	0.000	0.008	−6.745	−6.609
218	Ra	214	Rn	8.581	0.008	0.008	−4.585	−4.173
220	Ra	216	Rn	7.627	0.008	0.008	−1.638	−1.321
222	Ra	218	Rn	6.710	0.040	0.029	1.591	2.000
224	Ra	220	Rn	5.823	0.111	0.081	5.519	5.889
226	Ra	222	Rn	4.904	0.137	0.100	10.724	11.093

long as 1.2×10^7 s, but that of ^{212}Po is only 0.3 μs. This is directly related to the influence of the spherical shell closure at $N = 126$. Some typical results in this region are listed in Table I for the isotopic chains of Pb, Po, Rn, and Ra. In Table I, the mass numbers and chemical symbols of the parent nucleus and daughter nucleus are listed in columns 1–4. The α-decay energy Q_α is listed in column 5. The quadrupole deformation is given in column 6, and the hexadecapole deformation in column 7. The experimental and theoretical α-decay half-lives (in logarithm with a base 10) are given in columns 8 and column 9, respectively. As seen in Table I, we reproduce the half-lives of many α emitters within a factor of 2–3 in this region. The deviation between experiment and theory around the shell closure $N = 126$ can be further improved by combining the calculations of the cluster and microscopic models [50].

Because large deformations occur for many nuclei with $Z = 90$–100 and the influence of deformation on half-lives

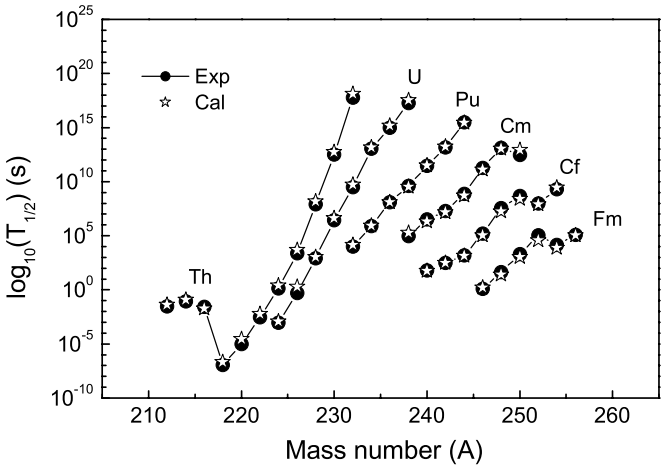

FIG. 4. Experimental and calculated α-decay half-lives for even-even isotopes of Th, U, Pu, Cm, Cf, and Fm.

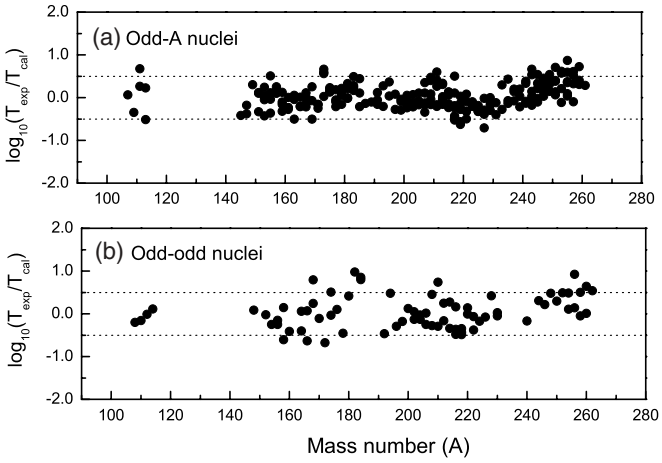

FIG. 5. Logarithms of the hindrance factors (HF $= T_{\mathrm{Exp.}}/T_{\mathrm{Cal.}}$) of odd-$A$ nuclei and odd-odd nuclei.

is evident, we compare the calculated half-lives with the measured ones for isotopes of Th, U, Pu, Cm, Cf, and Fm in Fig. 4. We see that the experimental data are well reproduced by DDCM in this deformed region. The theoretical points (stars) almost coincide with the experimental ones (black circles). In Fig. 4, the influence of the spherical shell closure $N = 126$ is clearly seen from the α decay half-lives of the Th isotopic chain. Around the spherical shell $N = 126$, the variation of experimental α decay half-lives of ^{216}Th ($N = 126$) and ^{218}Th ($N = 128$) is as large as 10^5 times. Around the deformed shell $N = 152$, the variation of half-lives is approximately 10 times for Cm, Cf, and Fm isotopic chains. For instance, the α-decay half-life of ^{252}Fm ($N = 152$) is only ten times larger than that of ^{254}Fm ($N = 154$). This demonstrates that the influence of the deformed shell on half-lives is less than that of the spherical one.

2. *Odd-A nuclei and odd-odd nuclei*

The situation of odd-A α emitters is more complicated than that of even-even nuclei. The ground-state spin and parity of odd-A nuclei cannot be automatically assigned as those of even-even nuclei. For some odd-A nuclei, the ground-state spin and parity are still unknown in experiment. The favored α transitions of these nuclei can either proceed to the ground state or to an excited state of the daughter nucleus. The ground-state to ground-state transition is not necessarily the favored case for odd-A α emitters. For odd-A and odd-odd nuclei, Audi *et al.* [51] pointed out that the assumption of favored transition is reasonable in regions where the Nilsson model for deformed nuclei applies. This assumption was often used to estimate the α-decay energy from nuclear masses by Audi *et al.* [51], and here we use the same assumption for deformed heavy nuclei [51]. Our calculations of odd A include 231 α emitters in the periodic table. The logarithms of average deviations of 231 odd-A nuclei are $S = \Sigma_{i=1}^{i=231}|\log_{10}T_{1/2}^{\mathrm{Exp.}}(i) - \log_{10}T_{1/2}^{\mathrm{Cal.}}(i)|/231 = 0.229$. This value of logarithm deviation corresponds to a factor of 1.8 between the experimental and theoretical half-lives. Because the half-lives of odd-mass nuclei vary erratically with neutron number, we also plot the logarithms of the hindrance factors (HF $= T_{\mathrm{Exp.}}/T_{\mathrm{Cal.}}$) of these nuclei in Fig. 5(a). The logarithms of the hindrance factors of odd-odd nuclei are plotted in Fig. 5(b), which we will discuss later. In Fig. 5(a), most of the points lie in the vicinity of the line HF $= 1.0$, which means the calculated lifetime is identical to the experimental one. For many odd-mass nuclei, the experimental half-lives are reproduced within a factor of 2. For some nuclei, the hinderance factor is beyond a factor of 3. These nuclei often involve very weak branch ratios of α decay and large uncertainties of experimental half-lives.

In Fig. 6, we further compare our predicted half-lives with the measured ones for odd-mass isotopes of the actinides ($Z = 89$–101). Fig. 6(a) is for odd-A nuclei with even proton numbers and Fig. 6(b) is for odd-A nuclei with odd proton numbers. The circle denotes the experimental partial half-life, and the star denotes the calculated one. We can see from Fig. 6 that the theoretical half-lives follow the experimental data well for both odd-even nuclei and even-odd nuclei. An analysis of Figs. 4–6 indicates that the deformed calculations reproduce well the experimental α-decay half-lives when large nuclear deformations are involved. This good agreement clearly shows the validity of the deformed DDCM for odd-A nuclei.

The α decay of odd-odd nuclei is slightly more complicated, and the available data are less than those of even-even nuclei and odd-A nuclei. We collect the 79 data of odd-odd α emitters in the region $Z = 53$–105 and calculate their half-lives with the deformed DDCM. The logarithms of average deviations of 79 odd-odd nuclei are $S = \Sigma_{i=1}^{i=79}|\log_{10}T_{1/2}^{\mathrm{Exp.}}(i) - \log_{10}T_{1/2}^{\mathrm{Cal.}}(i)|/79 = 0.318$. This value of logarithm deviation corresponds to a factor of 2.1 between the experimental half-life and theoretical one. For the details of calculated results, we plot the hindrance factors of the α-decay half-lives of these nuclei in Fig. 5(b). We see that the theoretical half-lives of many odd-odd α emitters are very close to the experimental data. We reproduce the half-lives of many odd-odd α emitters at the factor of 2–3 level. The half-lives of a few odd-odd α emitters are outside this range. Nevertheless

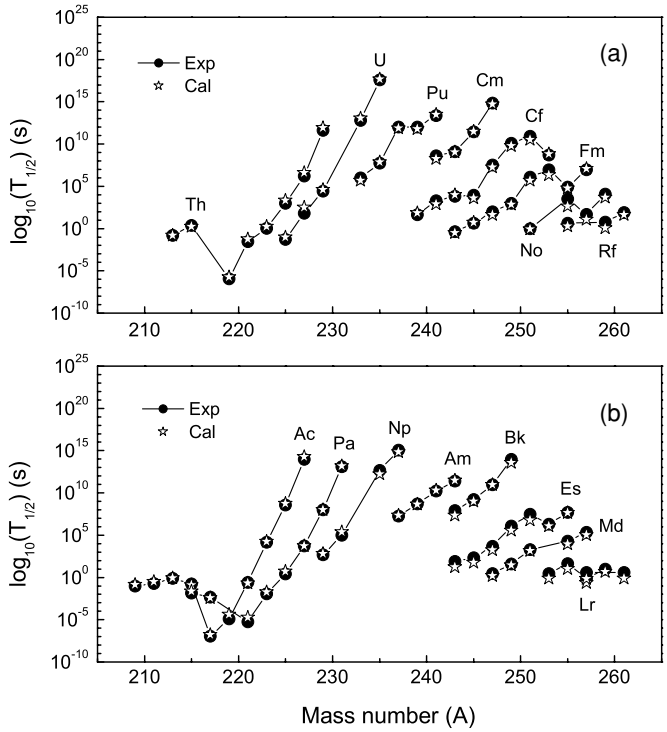

FIG. 6. Experimental and theoretical α-decay half-lives for odd-mass isotopes of actinides (89−101).

compared with previous calculations of odd-odd nuclei, the results of this article improve the agreement between theory and experimental data.

To see the overall agrement between the experimental data and theoretical results, we plot in Fig. 7 the average deviations between experiment and theoretical half-lives for three kinds of α emitters with proton number $Z = 52$–105. The logarithms of average deviations of even-even nuclei, odd-A nuclei, and odd-odd nuclei are $S_{ee} = 0.209$, $S_{oe} = 0.229$, and $S_{oo} = 0.318$, respectively. The logarithms of average deviations 0.3 and 0.5 corresponds to factors of 2.0 and 3.0 between experimental and theoretical half-lives. This implies that the experimental half-lives of even-even nuclei and odd-A nuclei are reproduced within a factor of 2 by the deformed DDCM. The average deviation of odd-odd α emitters is slightly larger than those of even-even and odd-A nuclei. However, the absolute deviation of the half-lives of odd-odd nuclei is also at the level of a factor of 2. This agreement between model and data is generally very good. A consistent treatment for both medium mass nuclei and heavy nuclei is obtained in a unified framework.

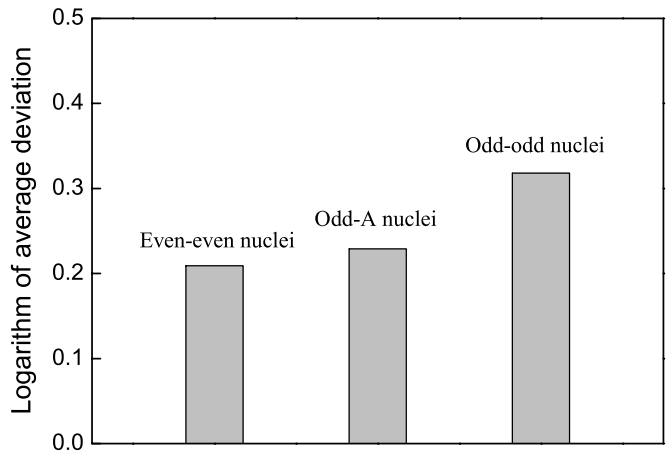

FIG. 7. Logarithms of average deviations (with a base 10) between experimental α-decay half-lives and theoretical ones for three kinds of nuclei.

3. *Superheavy nuclei*

There has been growing interest in the α-decay half-lives of superheavy nuclei in recent years [22,28,30,35,52,53]. These studies are useful for future experiments on superheavy nuclei. Based on the success of the deformed DDCM for nuclei with $Z = 52$–105, we now extend the calculations of half-lives to superheavy nuclei with $Z = 106$–110. In Table II, we give both the experimental α-decay half-lives and theoretical ones for isotopic chains of $Z = 106$–110 (Sg−Ds). The experimental α-decay energies Q_α are from [9,30] and listed in column 2. The quadrupole deformation in column 3 is taken from the calculations of the macroscopic-microscopic model (MM) [31]. The quadrupole deformation in column 4 is taken from the calculations of the relativistic mean-field model (RMF) with a TMA force parameter [52,53]. The experimental α-decay half-lives T_α(Exp.) [9,30] are given in column 5. The corresponding theoretical half-lives calculated by the two sets of deformation parameters (columns 6 and 7) are very close. The difference between the two sets of calculated half-lives is small. The logarithms of average deviations between the experiment half-lives and the two sets of calculated half-lives are 0.35 and 0.39, respectively, which correspond to a factor of 2.5 between the experimental and theoretical half-lives. The deformed calculations of DDCM also give reasonable results for the α-decay half-lives of nuclei in the superheavy region $Z = 106$–110. So we conclude that the agreement between the half-lives of DDCM and the data of superheavy nuclei is reached. For superheavy nuclei with $Z > 110$, there are large uncertainties in the deformation parameters used by the different theoretical models. On the experimental side, it would be interesting to improve the precision of experimental α-decay half-lives and to classify the decays from the ground state and from isomeric states. Therefore, the superheavy nuclei with $Z > 110$ are not included in the present deformed calculations, and it will be very interesting to investigate their properties in the future.

Before ending this section, let us quickly review the numerical results of the deformed DDCM. We calculated the α decay half-lives of many nuclei with proton number $Z = 52$–110. For the region of $Z = 52$–104, the number of even-even α emitters is 157 and the average deviation between the data and the theoretical results is within a factor of 2. The number of odd-A emitters in this region is 231, and the average deviation between the data and the theoretical results is also within a factor of 2. The average deviation of the α-decay half-lives of 79 odd-odd emitters in this region is

TABLE II. Experimental and theoretical α-decay half-lives of superheavy nuclei ($Z = 106$–110), in seconds.

Nuclei	Q_α(MeV)	β_2 MM	β_2 RMF	T_α(Expt)	T_α(Calc1) MM	T_α(Calc2) RMF
^{273}Ds $\rightarrow$ ^{269}Hs+α	11.291	0.231	0.220	1.1×10^{-4}	7.1×10^{-5}	7.8×10^{-5}
^{271}Ds $\rightarrow$ ^{267}Hs+α	10.958	0.230	0.230	6.2×10^{-4}	4.4×10^{-4}	4.4×10^{-4}
^{270}Ds $\rightarrow$ ^{266}Hs+α	11.242	0.230	0.240	1.0×10^{-4}	6.4×10^{-5}	5.9×10^{-5}
^{269}Ds $\rightarrow$ ^{265}Hs+α	11.345	0.230	0.240	2.7×10^{-4}	6.1×10^{-5}	5.6×10^{-5}
^{268}Mt $\rightarrow$ ^{264}Bh+α	10.299	0.229	0.250	7.0×10^{-2}	1.8×10^{-2}	1.5×10^{-2}
^{269}Hs $\rightarrow$ ^{265}Sg+α	9.354	0.229	0.220	7.1×10^{0}	1.7×10^{0}	1.8×10^{0}
^{267}Hs $\rightarrow$ ^{263}Sg+α	10.076	0.229	0.260	7.4×10^{-2}	1.7×10^{-2}	1.3×10^{-2}
^{266}Hs $\rightarrow$ ^{262}Sg+α	10.381	0.229	0.250	2.3×10^{-3}	1.8×10^{-3}	1.5×10^{-3}
^{265}Hs $\rightarrow$ ^{261}Sg+α	10.777	0.238	0.250	5.8×10^{-4}	2.9×10^{-4}	2.6×10^{-4}
^{264}Hs $\rightarrow$ ^{260}Sg+α	10.590	0.239	0.250	5.4×10^{-4}	5.4×10^{-4}	4.9×10^{-4}
^{267}Bh $\rightarrow$ ^{263}Db+α	9.009	0.229	0.260	1.7×10^{1}	8.6×10^{0}	6.4×10^{0}
^{266}Bh $\rightarrow$ ^{262}Db+α	9.477	0.229	0.260	1.0×10^{0}	6.4×10^{-1}	4.8×10^{-1}
^{265}Bh $\rightarrow$ ^{261}Db+α	9.380	0.228	0.260	9.4×10^{-1}	7.0×10^{-1}	5.2×10^{-1}
^{264}Bh $\rightarrow$ ^{260}Db+α	9.671	0.239	0.260	4.4×10^{-1}	1.8×10^{-1}	1.5×10^{-1}
^{266}Sg $\rightarrow$ ^{262}Rf+α	8.836	0.229	0.210	2.6×10^{1}	8.2×10^{0}	9.7×10^{0}
^{265}Sg $\rightarrow$ ^{261}Rf+α	8.949	0.228	0.220	2.4×10^{1}	6.0×10^{0}	6.4×10^{0}
^{263}Sg $\rightarrow$ ^{259}Rf+α	9.447	0.239	0.260	1.2×10^{-1}	1.8×10^{-1}	1.5×10^{-1}
^{261}Sg $\rightarrow$ ^{257}Rf+α	9.773	0.238	0.260	7.2×10^{-2}	2.4×10^{-2}	2.0×10^{-2}

approximately at a factor of 2. For the superheavy region with $Z = 106$–110, we calculated the half-lives of 18 α emitters, and the average deviation with the data is at a factor of 2.5. So the total number of α emitters investigated in this article is $N_{\text{Total}} = 157 + 231 + 79 + 18 = 485$. In 1993, Buck *et al.* [21] made a systematic study of α-decay half-lives of nuclei with $Z = 52$–109 by a spherical cluster model. In 2000, Royer [25] used the generalized liquid drop model to calculate the α-decay half-lives of 373 α emitters of which the numbers of even-even, odd-A, and odd-odd nuclei were 131, 192, and 50, respectively. After their calculations, some old data were corrected by experimental physicists and some new data of α-decay half-lives were obtained [1,2,51]. We have taken into account the corrections and added the new data in the calculations of this article [1,2,9,30,51]. Therefore, the number of α emitters in this article is 485, which covers the nuclei with $Z = 52$–110. This research is an important contribution to the study of α-decay half-lives. The global calculation of α-decay half-lives presented in this article should be useful in future studies of α-decay half-lives of medium and heavy nuclei far from stability and for those of superheavy elements. Finally, we would like to mention that there are other approaches to the study of α-decay of deformed nuclei [46–48]. Fröman [46] investigated α decay with the deformed WKB approach, and this was further developed by Delion *et al.* [47]. They successfully described the α decays of heavy and superheavy nuclei [47]. Recently, the α decay of actinides to rotational states has also been studied by the nonadiabatic approach with a double-folding potential, which explained well the partial half-lives of the first and second excited states [48,49]. This confirms again that the double-folding potential is successful for α-decay half-lives of nuclei and this conclusion agrees well with that of this article. In the calculations of this article, we took into account the α decays between the ground states of even-even nuclei and omitted the α decay to the first excited state of the rotational band of ground state in the daughter nucleus. According to previous studies, the transition to the first excited state of the rotational band can be omitted for spherical nuclei and for nuclei with moderate deformation [49,50]. But for well-deformed nuclei, the branching ratio to the first excited state can be as large as 20–30% because the excited energy of the first excited state is small [49,50]. This can bring the uncertainty in the calculated half-life to within the range 20–30%. However, the agreement between the calculated and experimental half-life is a factor of 2 or 3 (i.e., 200% or 300%), and one says that this is good agreement. Therefore, a 20–30% change in the half-life is small compared with 200% or 300%, and the omission of the transition to the first excited state does not influence the conclusion of this article. Actually, the transition to the first excited state can be included in the deformed DDCM, and there is no difficulty in including any nucleus if its excited energy of the first excited state is known [50]. But this involves a huge quantity of computational time for a systematic calculation of this study in which the number of nuclei is as large as 485 and the energy of the first excited state is still unknown for many nuclei such as those in the superheavy region. Of course, it will be interesting to pursue this problem further and to improve the agreement between the results of the model and the data.

IV. SUMMARY

In summary, we present a global calculation of α-decay half-lives for both even-A and odd-A nuclei with the deformed version of the density-dependent cluster model (DDCM), which considers nuclear deformations. The formulas for calculations of the α-decay half-lives are derived and presented in the deformed case of microscopic double-folding potentials. Detailed analysis for favored α transitions of nuclei with

$Z = 52$–110 is carried out in the deformed DDCM. The potentials between spherical α particles and deformed daughter nuclei are evaluated numerically from the double-folding model by the multipole expansion method. Based on the popular M3Y nucleon-nucleon interaction and the standard proton-proton Coulomb interaction, the α-core potentials in DDCM are well defined in physics. The nuclear deformations affect the barrier penetration probabilities significantly. The preformation factor used in the deformed DDCM is consistent for all nuclei in the nuclide chart. Their values are also in accord with the experimental facts and the microscopic calculations. The number of α emitters studied in this article is 485, and it covers the nuclei with $Z = 52$–110. So this is a global calculation of α-decay half-lives. The theoretical α-decay half-lives are in good agreement with the experimental data. A unified description of α-decay half-lives of both spherical and deformed nuclei is obtained by using the deformed density-dependent cluster model.

ACKNOWLEDGMENTS

Zhongzhou Ren thanks the following colleagues for fruitful discussions: Professors G. Münzenberg, S. Hofmann, M. Schädel, Yu. Ts. Oganessian, H. Q. Zhang, W. Q. Shen, G. O. Xu, G. M. Jin, Z. Qin, Z. G. Gan, J. S. Guo, and H. S. Xu. This work is supported by National Natural Science Foundation of China (No. 10125521, No. 10535010) and by 973 National Major State Basic Research and Development of China (No. G2000077400).

[1] G. Audi, O. Bersillon, J. Blachot, and A. H. Wapstra, Nucl. Phys. **A729**, 3 (2003).
[2] R. B. Firestone, V. S. Shirley, C. M. Baglin, S. Y. Frank Chu, and J. Zipkin, *Table of Isotopes*, 8th ed. (Wiley Interscience, New York, 1996).
[3] S. Hofmann and G. Münzenberg, Rev. Mod. Phys. **72**, 733 (2000).
[4] Yu. Ts. Oganessian *et al*., Phys. Rev. C **72**, 034611 (2005).
[5] T. N. Ginter *et al*., Phys. Rev. C **67**, 064609 (2003).
[6] A. Türler *et al*., Eur. Phys. J. A **17**, 505 (2003).
[7] R.-D. Herzberg, J. Phys. G **30**, R123 (2004).
[8] F. A. Danevich, A. Sh. Georgadze, V. V. Kobychev, S. S. Nagorny, A. S. Nikolaiko, O. A. Ponkratenko, V. I. Tretyak, S. Yu. Zdesenko, and Yu. G. Zdesenko, Phys. Rev. C **67**, 014310 (2003).
[9] Z. G. Gan, J. S. Guo, X. L. Wu, Z. Qin, H. M. Fan, X. G. Lei, H. Y. Liu, B. Guo, H. G. Xu, R. F. Chen, C. F. Dong, F. M. Zhang, H. L. Wang, C. Y. Xie, Z. Q. Feng, Y. Zhen, L. T. Song, P. Luo, H. S. Xu, X. H. Zhou, G. M. Jin, and Z. Ren, Eur. Phys. J. A **20**, 385 (2004).
[10] J. O. Rasmussen, in *Alpha-, Beta-, and Gamma-Ray Spectroscopy*, edited by K. Siegbahn (North Holland, Amsterdam, 1965), Vol. I, p. 701.
[11] Z. Ren and G. Xu, Phys. Rev. C **36**, 456 (1987).
[12] H. Horiuchi, Nucl. Phys. **A522**, 257c (1991).
[13] I. Tonozuka and A. Arima, Nucl. Phys. **A323**, 45 (1979).
[14] P. E. Hodgeson and E. Betak, Phys. Rep. **374**, 1 (2003).
[15] R. G. Lovas, R. J. Liotta, A. Insolia, K. Varga, and D. S. Delion, Phys. Rep. **294**, 265 (1998).
[16] G. Gamov, Z. Phys. **51**, 204 (1928).
[17] E. U. Condon and R. W. Gurney, Nature **122**, 439 (1928).
[18] N. Rowley, G. D. Jones, and M. W. Kermode, J. Phys. G **18**, 165 (1992).
[19] K. Varga, R. G. Lovas, and R. J. Liotta, Phys. Rev. Lett. **69**, 37 (1992).
[20] S. A. Gurvitz and G. Kalbermann, Phys. Rev. Lett. **59**, 262 (1987).
[21] B. Buck, A. C. Merchant, and S. M. Perez, At. Data Nucl. Data Tables **54**, 53 (1993).
[22] P. Mohr, Phys. Rev. C **73**, 031301(R) (2006).
[23] S. B. Duarte *et al*., At. Data Nucl. Data Tables **80**, 235 (2002).
[24] B. A. Brown, Phys. Rev. C **46**, 811 (1992).
[25] G. Royer, J. Phys. G **26**, 1149 (2000).
[26] G. Royer and R. A. Gherghescu, Nucl. Phys. **A699**, 479 (2002).
[27] D. N. Basu, Phys. Lett. **B566**, 90 (2003).
[28] Y. K. Gambhir, A. Bhagwat, and M. Gupta, Phys. Rev. C **71**, 037301 (2005).
[29] R. K. Gupta *et al*., Phys. Rev. C **65**, 024601 (2002).
[30] C. Xu and Z. Ren, Nucl. Phys. **A753**, 174 (2005); **A760**, 303 (2005).
[31] P. Möller, J. R. Nix, W. D. Myers, and W. J. Swiatecki, At. Data Nucl. Data Tables **59**, 185 (1995).
[32] S. Raman, C. H. Malarkey, W. T. Milner, C. W. Nestor, Jr., and P. H. Stelson, At. Data Nucl. Data Tables **36**, 1 (1987).
[33] Y.-J. Shi and W. J. Swiatecki, Nucl. Phys. **A464**, 205 (1987).
[34] T. L. Stewart, M. W. Kermode, D. J. Beachey, N. Rowley, I. S. Grant, and A. T. Kruppa, Nucl. Phys. **A611**, 332 (1996).
[35] V. Yu. Denisov and H. Ikezoe, Phys. Rev. C **72**, 064613 (2005).
[36] C. Xu and Z. Ren, Phys. Rev. C **73**, 041301(R) (2006).
[37] G. R. Satchler and W. G. Love, Phys. Rep. **55**, 183 (1979).
[38] H. J. Krappe, Ann. Phys. (NY) **99**, 142 (1976).
[39] M. J. Rhoades-Brown *et al*., Z. Phys. A **310**, 287 (1983).
[40] M. Ismail, A. Y. Ellithi, and F. Salah, Phys. Rev. C **66**, 017601 (2002).
[41] G. F. Bertsch, J. Borysowicz, H. Mcmanus, and W. G. Love, Nucl. Phys. **A284**, 399 (1977).
[42] A. M. Kobos, B. A. Brown, P. E. Hodgson, G. R. Satchler, and A. Budzanowski, Nucl. Phys. **A384**, 65 (1982).
[43] A. M. Kobos, B. A. Brown, R. Lindsay, and G. R. Satchler, Nucl. Phys. **A425**, 205 (1984).
[44] J. D. Walecka, *Theoretical Nuclear Physics and Subnuclear Physics* (Oxford University, Oxford, 1995), p. 11.

[45] B. Hahn, D. G. Ravenhall, and R. Hofstadter, Phys. Rev. **101**, 1131 (1956).
[46] P. O. Fröman, Mat. Fys. Skr. Dan. Vid. Selsk. **1**, 1 (1957).
[47] D. S. Delion, A. Sandulescu, and W. Greiner, Phys. Rev. C **69**, 044318 (2004).
[48] D. S. Delion, S. Peltonen, and J. Suhonen, Phys. Rev. C **73**, 014315 (2006).
[49] Y. A. Akovali, Nucl. Data Sheets **84**, 1 (1998).
[50] C. Xu and Z. Ren, Commun. Theor. Phys. **42**, 745 (2004) http://ctp.itp.ac.cn
[51] G. Audi, A. H. Wapstra, and C. Thibault, Nucl. Phys. **A729**, 129 (2003), p. 166.
[52] Z. Ren, F. Tai, and D.-H. Chen, Phys. Rev. C **66**, 064306 (2002); Nucl. Phys. **A722**, 543c (2003).
[53] Z. Ren, D.-H. Chen, F. Tai, H. Y. Zhang, and W. Q. Shen, Phys. Rev. C **67**, 064302 (2003); F. Tai, Ph.D. thesis, Nanjing University (2005).